SLOT DESIGN FOR DYNAMIC IRON LOSS REDUCTION IN INDUCTION MACHINES

Sana Jelassi[1, 2, 3], Raphael Romary[1, 2, *], and Jean-François Brudny[1, 2]

[1]Laboratoire Systèmes Electrotechniques et Environnement (LSEE), France

[2]Université d'Artois, Technoparc Futura, Béthune 62400, France

[3]Université Paris Grand Ouest, EPMI, France

Abstract—The goal of this paper is to present a semi analytical method which makes it possible the calculation of the dynamic iron losses in a three phase induction machine taking the slotting effect into account. The particularity of this method is that it allows the distinction of the stator and the rotor slot openings contribution in the dynamic and, consequently, in the total iron losses. This analytical study shows that a convenient choice of the stator and the rotor slot openings leads to an iron loss reduction, due to the cancellation of particular flux density slotting harmonics. Theoretical results are confirmed numerically.

1. INTRODUCTION

The satisfactory prediction of iron losses and their causes is a fundamental step in the design to insure high efficiency of AC rotating machines [1, 2]. Consequently, estimation of the machine losses becomes an issue of great concern for electric-motor designer [3] who is forced to propose optimal designs with low time computing methods. In AC machines, the study are mainly devoted to the estimation of the iron losses due to non sinusoidal supply with a PWM inverter [4, 5]. But actually, in addition to the **F**lux **D**ensity (**FD**) components which originate from the supply, harmonic components, generated mainly by the slotting effect, exist in the air-gap. Their impact on the vibratory and acoustic behaviour is well known. Reduction procedures,

based on the knowledge of the slotting effect phenomenon, have been developed [6, 7]. These **FD** components affect also the iron losses. However, in the literature, the corresponding studies are rather few although experiments studies carried out on an induction machine, conclude on the non negligible impact of this phenomenon on the stator and the rotor dynamic iron losses. This result has been confirmed using FEM software [8] or analytical developments [9]. The iron loss reduction can be achieved using another material that constitutes the stator and rotor magnetic circuit as presented in [10] where grain oriented steel is used. Nevertheless, the procedure needs a special arrangement of the laminations [11].

The aim of this paper is to show how to optimize the design of the induction machine slots with regard to dynamic iron loss reduction considering a convenient choice of the slot openings. The study considers a sine supply. The approach determines first, analytically, the **FD** distribution in the stator and rotor cores from the air-gap **FD**. Then, a simple model, which is used to characterize the iron losses is numerically exploited. This semi analytical model makes it possible to quickly evaluate the iron losses, and show the importance of the stator and rotor slot openings for the dynamic iron loss minimization. A numerical study is then carried out to validate the theoretical results.

2. AIR-GAP FLUX DENSITY

The various variables will be labelled with the superscript "s" for the stator or "r" for the rotor. In this study, a three phase ($q = 3$), p pole pair squirrel cage induction machine with N^s stator slots and N^r rotor bars per pole pair is considered. As the number of rotor bar can be non multiple of the pole pair number, N^r may be non-integer. All the q phase coils are series connected. The stator is supplied by a v_q^s three phase balanced sinusoidal voltage system of ω angular frequency (frequency f). The rotor bar induced currents include the fundamental at sf frequency (s is the slip) and harmonics. These currents will created their own magnetic effects but according to the Lenz law, the flux density components generated by the rotor will tend to be opposed to the cause which gives rise to them. This is called the magnetic armature reaction. However, if the stator currents are assumed to be sinusoidal, the magnetic armature reaction is not completely realized because some rotor **FD** components do not find their equivalent in the ones generated by the stator. That will induce harmonic currents in the stator winding which will generate the missing stator **FD** components. Thanks to these stator harmonic currents, all the **FD** components generated by the rotor are compensated and the

magnetic armature reaction is satisfied for all the rotor and stator components. Consequently, only the effects generated by the no load $i^s_{q(0)}$ fundamental stator currents of $I^s_{(0)}$ rms value are considered. This is enough to define the b^g air-gap flux density harmonic content. b^g is calculated by multiplying the ε air-gap magnetomotive force (mmf) generated by the stator winding by the Λ per area unit air-gap permeance which takes the slotting effect into account. The air-gap permeance model is based on rectangular slots shape and considers radial the field lines in the air-gap. However, practically, the field lines do not join the bottom of the slots. Consequently, in order to express Λ, fictitious slots depth equal to the fifth of their openings [12] have to be considered. Denoting g the air-gap thickness, Λ is defined as μ_0/g and the Fourier series decomposition of this quantity leads to the following expression for Λ:

$$\Lambda(\alpha^s, \theta) = \sum_{k_s=-\infty}^{+\infty} \sum_{k_r=-\infty}^{+\infty} \Lambda_{k_s k_r} \cos\left((k_s N^s + k_r N^r)p\alpha^s - pk_r N^r \theta\right) \quad (1)$$

k_s and k_r are positive, negative or null integers. α^s is the angular abscissa of any point in the air-gap related to the stator referential d^s, confounded with the phase 1 axis as presented in Fig. 2. θ represents the angular position, relatively to d^s, of the rotor referential d^r tied with the rotor tooth 1 axis. When the machine rotates at given s, θ can be expressed as:

$$\theta = (1-s)\,\omega t/p \quad (2)$$

$\Lambda_{k_s k_r}$ is defined as follows:

$$\Lambda_{kskr} = \mu_0 A_{sr} f(k_s) f(k_r) \quad (3)$$

$f(k_s)$ and $f(k_r)$ are the stator and rotor slotting functions expressed by:

$$\left.\begin{array}{l} f(k_s) = \frac{\sin(k_s r^s_t \pi)}{2k_s} \\ f(k_r) = \frac{\sin(k_r r^r_t \pi)}{2k_r} \end{array}\right\} \quad (4)$$

A_{sr} depends on the slot geometry and g_m, the minimal air-gap thickness. r^s_t and r^r_t are the slotting ratio given respectively by: $r^s_t = w^s_t/(w^s_t + w^s_s)$ and $r^r_t = w^r_t/(w^r_t + w^r_s)$. $w^{s,r}_s$ and $w^{s,r}_t$ represent the width of respectively one slot and one tooth. These parameters are presented in Fig. 1. Let us point out that for k_s and (or) $k_r = 0$, Equation (3) is still valid on condition to take $f(k_s)$ and (or) $f(k_r) = 1$.

If at $t = 0$ the current $i^s_{1(0)}$ is maximum, ε is given by:

$$\varepsilon = \sum_{h^s} \hat{\varepsilon}_{h^s} \cos\left(\omega t - h^s p\alpha^s\right) \quad (5)$$
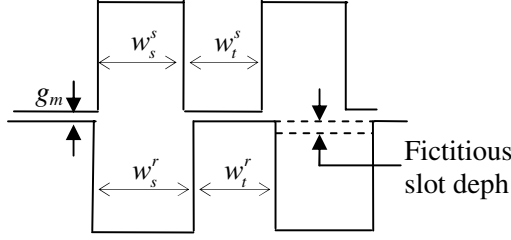
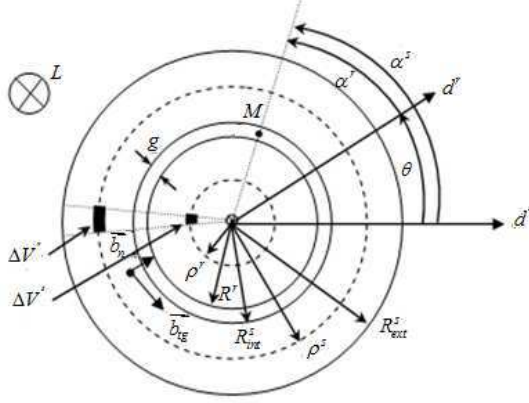**Figure 1.** Stator and rotor slots and teeth.

Figure 2. Machine geometry.

where:

$$\hat{\varepsilon}_{h^s} = \frac{n^s \sin(h^s(1 - r_t^s)\pi/pN^s)}{\sqrt{2}m^s\pi(h^s)^2(1 - r_t^s)\pi/pN^s} I_{(0)}^s \tag{6}$$

n^s is the turns number per phase per pole pair. m^s represents the slots number per phase per pole. h^s is a positive or negative integer which characterizes the mmf space harmonic: $h^s = 6k + 1$, where k can takes positive, negative or null values. These quantities define b^g which can be expressed in a stator referential as:

$$b^g = \sum_{h^s,k_s,k_r} \hat{B}_{h^s k_s k_r}^g \cos\left(\omega t + pk_r N^r \theta - p\left(h^s + k_s N^s + k_r N^r\right)\alpha^s\right) \tag{7}$$

Introducing (2), b^g given by (7) becomes:

$$b^g = \sum_{h^s,k_s,k_r} \hat{B}_{h^s k_s k_r}^g \cos(K^s \omega t - G\alpha^s) \tag{8}$$

The K^s frequency rank and the G pole pair number of an elementary

FD component are defined as:

$$\left. \begin{array}{c} K^s = 1 + k_r N^r (1-s) \\ G = p\left(h^s + k_s N^s + k_r N^r\right) \end{array} \right\} \tag{9}$$

3. FLUX DENSITY REPARTITION

The **FD** variations in the air-gap will be refund in the stator and rotor iron parts of the machine, generating iron losses. Consequently, iron loss estimation requires a model that provides the **FD** repartition in the stator and the rotor iron. To characterize these **FD** repartitions, a simplified smooth air-gap machine is considered as shown in Fig. 2, where the main used notations are specified. The $\vec{b}_n$ normal and $\vec{b}_{tg}$ tangential **FD** components in each ΔV^s and ΔV^r elementary volume, characterized respectively by their distance ρ^s and ρ^r from the O machine axis are also presented. Although the eddy currents in the stator and rotor cores are the cause of the dynamic losses, it will be assumed that they have no magnetic effect [13]. This is due to the insulation between laminations that limits their circulation. So they are not considered in the equations used to determine the flux density distribution. In order to determine analytically b_n and b_{tg}, the following equations have to be solved:

$$\left. \begin{array}{c} div\vec{b} = 0 \\ \overrightarrow{curl}\vec{h} = 0 \end{array} \right\} \tag{10}$$

Boundary conditions at the stator and rotor interfacing surfaces (flux density normal component and magnetic field tangential component conservation) are used to determine analytically b_n and b_{tg}, assuming that b^g given by (8), is imposed in the ideal air-gap of constant thickness. Solutions of this kind of problem are presented in [14].

If one component at given G is considered, the relative variations of $\hat{B}_n$, $\hat{B}_{tg}$ magnitudes in the stator: $\hat{B}_n^s(\rho^s)/\hat{B}_n^s(\rho^s = R_{int}^s)$, $\hat{B}_{tg}^s(\rho^s)/\hat{B}_{tg}^s(\rho^s = R_{int}^s)$ and in the rotor: $\hat{B}_n^r(\rho^r)/\hat{B}_n^r(\rho^r = R^r)$ = $\hat{B}_{tg}^r(\rho^r)/\hat{B}_{tg}^r(\rho^r = R^r)$, are given in Fig. 3 for different values of G and for $R_{int}^s = 60\,\text{mm}$, $R_{ext}^s = 90\,\text{mm}$, $R^r = 59.5\,\text{mm}$, $g = 0.5\,\text{mm}$ and $L = 170\,\text{mm}$. It can be observed that the more G increases, the less the **FD** penetrates inside the iron, reducing the volume of iron concerned by losses. For $G = 1$, The relative values of $\hat{B}_n$ and $\hat{B}_{tg}$ are constant. In this case there is no attenuation along the rotor frame because the flux lines cross through the rotor.
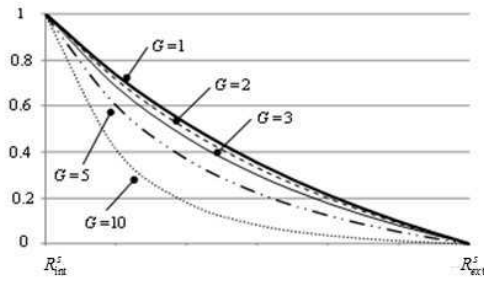
(a) Relative variations of $\hat{B}_n^s$ with ρ^s.
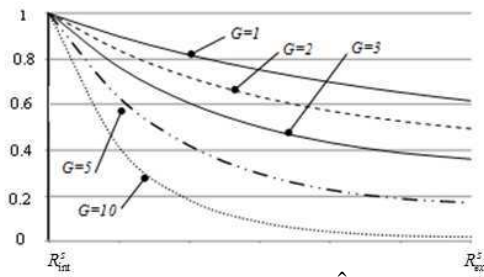
(b) Relative variation of $\hat{B}_{tg}^s$ with ρ^s
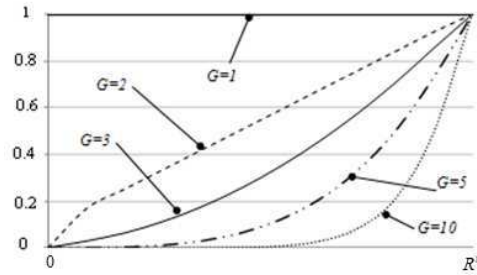
(c) Relative variations of $\hat{B}_n^r$ and $\hat{B}_{tg}^r$ with ρ^r

Figure 3. Relative variations of the stator and the rotor **FD**.

4. IRON LOSS ANALYSIS

4.1. Iron Loss Model

The separation of iron losses corresponds to a subdivision in static losses, dynamic losses and excess losses [15]. Static losses are caused by friction of the magnetic domains. Dynamic losses (eddy current) are related to the magnetic field variations which induce currents in the conductive metallic mass causing energy dissipation [16]. Excess losses are caused by the local eddy currents induced by the magnetic

domains movement [17]. In the case of non sine excitation, only the dynamic losses verified the principle of superposition. Within the frame of that study, the harmonic contribution on the static losses will be neglected. Actually, as the **FD** harmonic magnitudes due to the slotting effect are less than a hundredth of the fundamental one, it is possible to neglect the secondary loops which intervene in the static loss calculation. Concerning the excess losses, they can be characterized in more complex form [18] based on the **FD** real waveform knowledge. So this work will be focused only on the dynamic iron losses caused by eddy currents flowing in the laminations. In AC electrical rotating machine, the complexity of the phenomena related to the slotting effect, requires, for the analytical study, to use a simplified iron loss model. However it can be expected that the tendencies which will be highlighted on the dynamic losses are the same concerning the excess losses. Let us consider first that the ΔV^s elementary volume is excited by a sinusoidal, f frequency, $\hat{B}_1^s$ magnitude **FD**. The $\Delta P_{d(f)}^s$ dynamic iron losses generated in ΔV^s elementary volume are expressed by:

$$\Delta P_{d(f)}^s = C_d^s f^2 \hat{B}_1^{s^2} \tag{11}$$

$\hat{B}_1^s$ is the **FD** component magnitude corresponding to $K^s = 1$ and resulting from the summation of all the **FD** waves of same f frequency and with different pole pair numbers. $\hat{B}_1^s$ is defined by: $\hat{B}_1^s = \sqrt{\hat{B}_{1n}^{s}{}^2 + \hat{B}_{1tg}^{s}{}^2}$ where $\hat{B}_{1n}^s$ and $\hat{B}_{1tg}^s$ are respectively the **FD** normal and tangential component magnitudes. In each ΔV^r elementary volume, the dynamic iron losses due to the fundamental are expressed by:

$$\Delta P_{d(sf)}^r = C_d^r s^2 f^2 \hat{B}_1^{r^2} \tag{12}$$

C_d^s and C_d^r are coefficients which depend on the magnetic circuit weight, the conductivity as well as other factors. $\hat{B}_1^r$ is defined by $\hat{B}_1^r = \sqrt{\hat{B}_{1n}^{r}{}^2 + \hat{B}_{1tg}^{r}{}^2}$. The total dynamic iron losses due to the fundamental **FD** are given by:

$$P_{d(f)} = P_{d(f)}^s + P_{d(sf)}^r \tag{13}$$

$P_{d(f)}^s$ and $P_{d(sf)}^r$ are obtained respectively by summing numerically $\Delta P_{d(f)}^s$ and $\Delta P_{d(sf)}^r$ generated by all the ΔV^s and ΔV^r elementary volumes that constitute the stator and the rotor cores presented in Fig. 2. In induction machines, the presence of K^s stator and K^r rotor rank harmonic **FD** components, with $\hat{B}_{K^s}^s$ and $\hat{B}_{K^r}^r$ magnitudes [19], superposed to the fundamental wave, require the use of an iron loss model that takes into account non sinusoidal excitation. $\hat{B}_{K^s}^s$ and

$\hat{B}^r_{K^r}$ are also obtained by summation of elementary **FD** components of different pole pair number. K^r is deduced from K^s by considering (8) expressed in the d^r referential using α^r as the angular abscissa of any point in the air-gap: $\alpha^r = \alpha^s - \theta$. K^r is given by:

$$K^r = 1 - (h^s + k_s N^s)(1 - s) \tag{14}$$

The extension of the model given by (11) and (12) allows defining the dynamic harmonic iron losses as follows [20]:

$$\Delta P^s_{d(harm)} = \sum_{K^s=2}^{\infty} \Delta P^s_{d(K^s f)} = C^s_d f^2 \hat{B}^{s^2}_1 \sum_{K^s=2}^{\infty} \left(\frac{\hat{B}^s_{K^s}}{\hat{B}^s_1}\right)^2 K^{s^2} \tag{15}$$

$$\Delta P^r_{d(harm)} = \sum_{K^r=2}^{\infty} \Delta P^r_{d(K^r f)} = C^r_d f^2 \hat{B}^{r^2}_1 \sum_{K^r=2}^{\infty} \left(\frac{\hat{B}^r_{K^r}}{\hat{B}^r_1}\right)^2 K^{r^2} \tag{16}$$

$\Delta P^s_{d(K^s f)}$ and $\Delta P^r_{d(K^r f)}$ are the dynamic iron losses, due respectively to K^s and K^r rank harmonic **FD** components, in each iron elementary volume. The total dynamic iron losses due to the harmonic **FD** are given by:

$$P_{d(harm)} = P^s_{d(harm)} + P^r_{d(harm)} \tag{17}$$

$P^s_{d(harm)}$ and $P^r_{d(harm)}$ are also obtained by summation of the losses $\Delta P^s_{d(harm)}$ and $\Delta P^r_{d(harm)}$ on the whole stator and rotor cores. The total dynamic iron losses are expressed by:
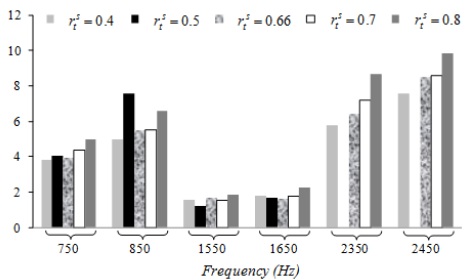
$$P_d = P_{d(f)} + P_{d(harm)} \tag{18}$$
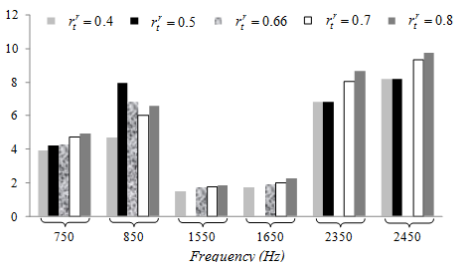
4.2. Numerical Applications

The numerical applications are realized considering two three-phase squirrel induction machines.

Machine I: 11 kW, 380/660 V, 50 Hz. This machine is characterized by: $p = 2$, $N^s = 24$, $N^r = 16$. The values of r^s_t and r^r_t are adjusted by changing w^s_s, w^r_s, w^s_t and w^r_t. The other dimensions of the machine remain constant but the air-gap fundamental **FD** magnitude is kept constant at 1 T by adjusting $I^s_{(0)}$. The used iron loss model allows decomposing the contribution of each harmonic **FD** as far as the dynamic losses are concerned. $P^r_{d(sf)}$ are null because $s \approx 0$, so $P_{d(f)} = P^s_{d(f)}$.
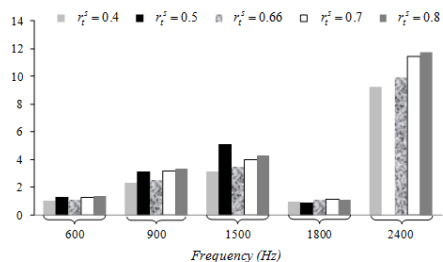
For this machine, Fig. 4 gives the percentage (in percent) of $P^s_{d(K^s f)}$ and $P^r_{d(K^r f)}$ relatively to $P_{d(f)}$ for various combinations of r^s_t and r^r_t. It can be noticed that the components at 2350 Hz and 2450 Hz (Figs. 4(a) and 4(b)) in the stator referential and their homologues at
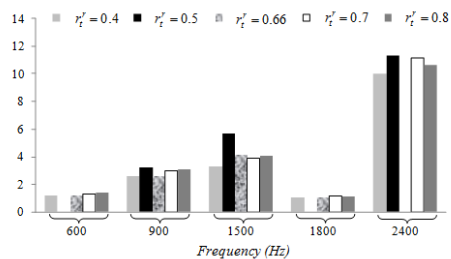
(a) The ratio $P^s_{d(K^sf)} / P_{d(f)}$ (in percentage) for $r^r_t = 0.8$

(b) The ratio $P^s_{d(K^sf)} / P_{d(f)}$ (in percentage) for $r^s_t = 0.8$

(c) The ratio $P^r_{d(K^rf)} / P_{d(f)}$ (in percentage) for $r^r_t = 0.8$

(d) The ratio $P^r_{d(K^rf)} / P_{d(f)}$ (in percentage) for $r^s_t = 0.8$

Figure 4. Percentage of $P^s_{d(K^sf)}$ and $P^r_{d(K^rf)}$ relatively to $P_{d(f)}$ for $N^s = 24$ and $N^r = 16$.

2400 Hz (Figs. 4(c) and 4(d)) in the rotor referential have an important contribution in the dynamic losses for $r_t^s \neq 0.5$ and $r_t^r \neq 0.66$. These components correspond to $G = p$, so $h^s = 1$ and $k_s N^s + k_r N^r = 0$, leading to: $|k_s N^s| = |k_r N^r|$. This particularity corresponds to the slotting resonance phenomenon [21]. According to the machine parameters, these conditions are satisfied for $|k_s| = 2$ and $|k_r| = 3$ leading to $K^s = 47$ and $K^s = 49$ so $f = 2350\,\text{Hz}$ and $f = 2450\,\text{Hz}$ in the stator referential and $K^r = 48$ so $f = 2400\,\text{Hz}$ in the rotor referential. These components of low pole pair numbers spread on a more important area in the stator and the rotor cores than the components of higher polarity. In the particular case corresponding to $r_t^s = 0.5$ or $r_t^r = 0.66$, the contribution of the 2350 Hz, 2400 Hz and 2450 Hz harmonics in the iron losses is null. That property can be accounted for considering (3) and (4) which show that the corresponding $\hat{B}_{h^s k_s k_r}^g$ **FD** component can be cancelled through the $f(k_s)$ and $f(k_r)$ functions: $f(k_s = \pm 2) = 0$ for $r_t^s = 0.5$ and $f(k_r = \pm 3) = 0$ for $r_t^r = 0.66$. When $r_t^r = 0.5$, $f(k_r = \pm 2) = 0$, so the **FD** components at 1550 Hz and 1650 Hz in the stator referential are null as well as the corresponding dynamic iron losses. Let us point out that each component at given K^s or K^r results actually from several elementary components of different G. In Table 1, the percentage of $P_{d(harm)}$ relatively to P_d versus r_t^s and r_t^r are presented. It can be observed that there is an optimal value of r_t^s and r_t^r which gives the minimum of $P_{d(harm)}$: $r_t^s = r_t^r = 0.5$. In this case, the contribution of the **FD** harmonics at 1550 Hz, 1650 Hz, 2350 Hz and 2450 Hz in the stator referential and those at 700 Hz, 2200 Hz and 2400 Hz in the rotor referential is null and the iron losses are the lowest. r_t^s and r_t^r have an important role to reduce the iron losses in rotating electrical machines. Indeed, by adjusting their values, $P_{d(harm)}$ can be decreased by almost 31% (difference between the case where $r_t^s = r_t^r = 0.5$ and that corresponding to $r_t^s = r_t^r = 0.8$) as shown in Table 1. This

Table 1. Percentage of $P_{d(harm)}$ relatively to P_d for $N^s = 24$ and $N^r = 16$.

r_t^r	r_t^s				
	0.4	**0.5**	**0.66**	**0.7**	**0.8**
0.4	16.23	12.57	19.64	26.81	31.62
0.5	25	**4.9**	27.8	17.6	20
0.66	11.24	8.81	15.25	29.3	32.3
0.7	28.5	18.9	29.7	32.8	34.3
0.8	30	21	32.2	33.4	35.7

result proves that to minimize the iron losses, it is necessary to choose adequately the slot opening. Moreover, as far as the results presented in [7] are concerned, it can be pointed out that a correlation exists between magnetic noise and iron losses in rotating electrical machines.

Machine II: the second machine is characterized by: $p = 2$, $N^s = 18$, $N^r = 14$. For this machine, Table 2 gives, the percentage of $P_{d(harm)}$ relatively to P_d versus r_t^s and r_t^r. In this case the optimum r_t^s and r_t^r value which gives the minimum of $P_{d(harm)}$ are: $r_t^s = 0.66$ and $r_t^r = 0.4$. Indeed, for this machine, **FD** harmonics due to $|k_s| = 3$ and $|k_r| = 4$ have the most important contribution in the iron losses. Contrary to the previous machine, this combination does not lead to $k_s N^s + k_r N^r = 0$ but this quantity becomes minimum (± 2), leading to $G = 3p$ and $G = -p$ when $h^s = 1$. The contribution if these **FD** harmonics can be cancelled by choosing $r_t^s = 0.66$ because for this value it comes $f(k_s) = 0$. In this case, the choice of r_t^s can decrease the iron losses due to the **FD** harmonic by almost 34% as shown in Table 2.

Table 2. Percentage of $P_{d(harm)}$ relatively to P_d for $N^s = 18$ and $N^r = 14$.

r_t^r	r_t^s				
	0.4	0.5	0.66	0.7	0.8
0.4	16.84	21.23	**5.4**	24.32	28.25
0.5	18.65	23.68	12.62	28.25	33.47
0.66	22.82	28.44	17.73	32.63	35.61
0.7	26.65	31.52	21.41	33.38	37.32
0.8	29.74	33.66	24.35	35.84	38.85

Experimental checking of the properties concerning the slot opening is not easy to perform because it requires at least two identical machines with different slot opening. However, an experimental analysis presented in [9], based on the measurement of the torque generated by the eddy currents that flow in the iron allows one to provide information about the amount of dynamic losses generated by the slotting harmonic flux density. The results presented in that paper are in good accordance with the theoretical results presented in this one.

5. FINITE ELEMENT METHOD

The analytical analysis is based on several hypotheses concerning the air-gap permeance (see Section 2) and the **FD** repartition in the stator

and the rotor cores (see Section 3). The aim of the finite element
analysis is to check that the properties displayed in the analytical
development are still valid in case of real slot geometry where the
previous hypotheses are not considered. The presented numerical
analysis is focused on the possibility to cancel the **FD** components tied
to the slotting resonance phenomenon through a convenient choice of
r_t^s and r_t^r.

5.1. Problem Description

A numerical study based on finite element analysis provides space
variation or time variation of the **FD** at any point in the machine core.
A Fourier analysis can be performed on these variations to determine
the harmonic magnitudes. Nevertheless, a deep analysis destined
to compare analytical and simulation results is difficult because in
the analytical approach each harmonic is composed of the sum of
several elementary components of magnitude $\hat{B}_{h^s k_s k_r}^g$ which cannot
be identified separately. Taking for example the **FD** given by (7),
at given α^s, the time harmonic ranks depend on k_r, but at given
k_r, it is necessary to sum all the components of magnitude $\hat{B}_{h^s k_s k_r}^g$
resulting from h^s and k_s variations. In that numerical study, one
will be interested on the slotting resonance components corresponding
to $h^s = 1$, and $k_s N^s + k_r N^r = 0$. An additional difficulty of the
analysis concerns the magnitude of these components which are low
compared to the fundamental magnitude obtained for $k_r = 0$ ($\approx 1\%$ of
the fundamental) and the previous harmonics ($k_r = \pm 1, \pm 2 \ldots$) ones.

Nevertheless, as these components have low pole pair numbers
($G = 1$), a method based on the properties concerning the attenuation
of the components in the stator yoke, as presented in Fig. 2, will be
exploited.

5.2. Methodology and Simulation Principle

A simplified two pole three phase machine with reduced number of
slots is considered: $N^s = 12$, $N^r = 8$. Of course, such a machine is not
realistic but the aim is not to model a real machine but to verify the
analytical properties concerning the cancellation of some **FD** harmonic
by an convenient choice of r_t^s and r_t^r. In order to simplify the analysis,
only the stator is supplied with constant currents ($\omega = 0$), to eliminate
the time variation of the fundamental (K^s, $G = 1$): $i_{1(0)}^s = \sqrt{2} I_{(0)}^s$ and
$i_{2(0)}^s = i_{3(0)}^s = -\frac{\sqrt{2} I_{(0)}^s}{2}$ that correspond to $t = 0$. The simulation is done
in linear magneto-static with different rotor positions: θ varies from

0 to 45° that corresponds to one rotor slot pitch, with a calculation step of 1.25°. In order to put into play the attenuation properties of the **FD** components, the value of the **FD** normal component will be picked up at a location very close to the stator periphery ($\rho^s \approx R_{ext}^s$). This location corresponds to the point P in the d^s axis shown in Fig. 7, which corresponds to $\alpha^s = 0$. It will be supposed that the harmonics of high pole pair numbers are strongly attenuated and remains only the components of low attenuation such as $G = 1$. In these conditions, the analytical formulation leads to define the normal **FD** at the point P as following:

$$b_{n(P)}^s = \sum_{k_r} C_1 \hat{B}_{k_r}^s \cos(pk_r N^r \theta) \tag{19}$$

C_1 is the attenuation coefficient through the full stator yoke (see Fig. 3) related to b_n^s and the magnitude $\hat{B}_{k_r}^s$ is defined as:

$$\hat{B}_{k_r}^s = \sum_{h^s, k_s} \hat{B}_{h,^s k_s, k_r}^s \tag{20}$$

where h^s, k_s, k_r verify the condition $h^s + k_s N^s + k_r N^r = 1$. As previously mentioned, the slotting resonance harmonics are defined for $h^s = 1$, $k_s = \pm 2$ and $k_r = \pm 3$. As $\hat{B}_{1,2,-3}^s = \hat{B}_{1,-2,3}^s$, their contribution to the normal **FD** at the point P can be expressed as following:

$$b_{n(P),|k_r|=3}^s = 2C_1 \hat{B}_{1,-2,3}^s \cos(24\theta) \tag{21}$$

Equation (21) shows that $b_{n(P),|k_r|=3}^s$ spatial period is equal to $\pi/12$. For the numerical analysis, two slots shapes are treated. In the first case, rectangular slots corresponding to the ideal model used in the analytical developments are studied (Fig. 5(a)). In the second case, semi-closed slots are considered (Fig. 5(b)). For each slot shape two cases are treated, first $r_t^s = r_t^r = 0.8$ then $r_t^s = 0.5$ and $r_t^r = 0.8$. Fig. 5 gives also the geometrical parameters used to define r_t^s and r_t^r. For the

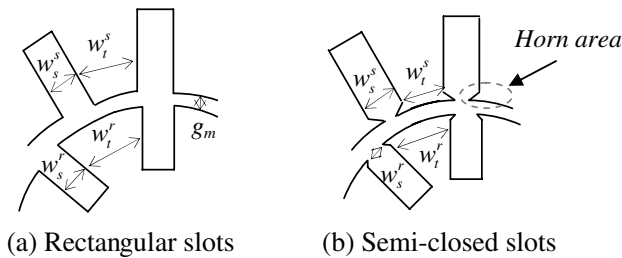(a) Rectangular slots   (b) Semi-closed slots

Figure 5. Slots shape.

semi-closed slot, the horn area is generally saturated. Consequently, it is not suitable to consider the geometrical parameters w_s^s, w_t^s, w_s^r, w_t^r at the level of the air-gap for the analytical model.

5.3. Simulation Results

The Maxwell finite element software is used. The studied machine is introduced into an infinite box verifying the following boundary condition: at $x \to \infty$ the FD is null. Starting with the rectangular slots where $r_t^s = r_t^r = 0.8$, the flux lines are presented in Fig. 6. According to the flux lines path, it can be observed that the d^s axis is not exactly in the polar axis, as it should be with the considered simulation conditions. Actually the rotor slots shift the polar axis; this phenomenon does not appear in the analytical model. Let us denote $b_{n(P)}^{s*}$ the normal **FD** at the point P resulting from the numerical simulation. $b_{n(P)}^{s*}$ versus θ is given in Fig. 7. Fig. 8 gives the **FD**
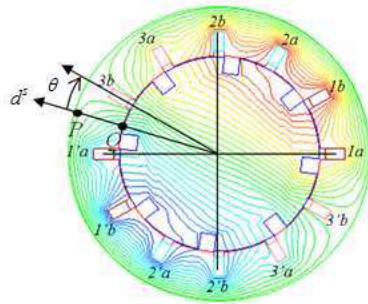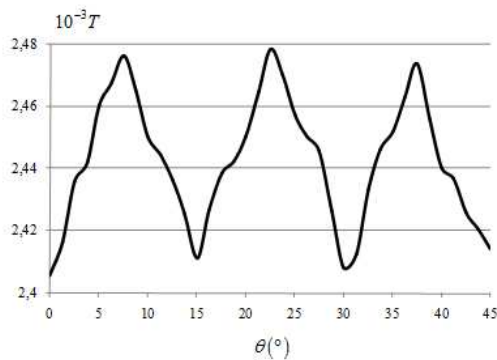

Figure 6. Flux lines for rectangular slots.

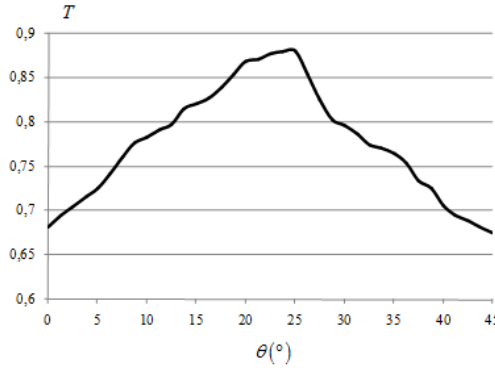**Figure 7.** $b_{n(P)}^{s*}$ for $r_t^s = r_t^r = 0.8$ for rectangular slots.

Figure 8. $b^{g*}_{(Q)}$ for $r^s_t = r^r_t = 0.8$ for rectangular slots.

calculated at the level of Q in the air-gap (Fig. 6), denoted $b^{g*}_{(Q)}$. It can be noticed that $b^{s*}_{n(P)}$ may be considered as periodic with $\pi/12$ period, that mean that it mainly originates from the slotting resonance harmonic given by (20). The mean value $(2.44 * 10^{-3}\,\text{T})$ corresponds to the fundamental obtained for $k_r = 0$ and $G = 1$. The variation of $b^{s*}_{n(P)}$ around its mean value can be used to identify the magnitude of $b^s_{n(P),|k_r|=3}$. As the fundamental is affected by the same attenuation, one can conclude that the magnitude of the slotting resonance harmonics, $\hat{B}^s_{1,2,-3}$ and $\hat{B}^s_{1,-2,3}$ represents approximately 1.4% of the fundamental. In Fig. 8, one can observe a curve of $\pi/4$ period corresponding to the first slotting harmonics ($k_r = \pm 1$) present in the air-gap. Moreover, its relative magnitude is higher (more than 10% of the fundamental). The comparison between these two curves allows one to highlight that the slotting resonance harmonics spread on a more important area than other slotting harmonics of higher polarity, strongly attenuated. The numerical study shows that the fundamental **FD** corresponding to $G = 1$ is attenuated by 0.3% along the stator yoke. This result is in agreement with the analytical one presented in Section 3.

Let us consider now the case of $r^s_t = 0.5$ and $r^r_t = 0.8$. The $b^{s*}_{n(P)}$ computation leads to the curve given in Fig. 9. This curve is different from the curve of Fig. 7. Indeed, $b^{s*}_{n(P)}$ is almost constant in this case. The variation which indicates the presence of the slotting resonance harmonics is almost null. The variations that still remain correspond to the second order slotting resonance harmonics ($k_r = \pm 6$). $b^{g*}_{(Q)}$ is given by Fig. 10. One can observe that the variations in the air-gap are reduced too. Theoretical results concerning the cancellation of the
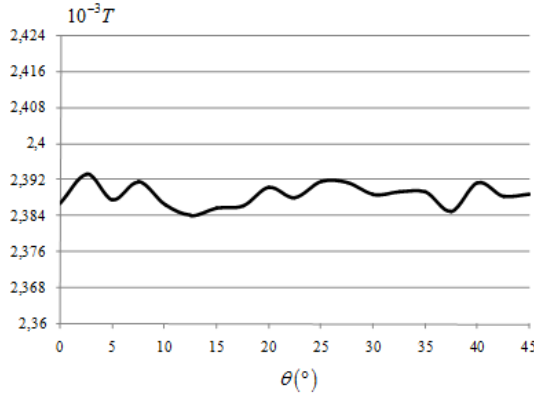
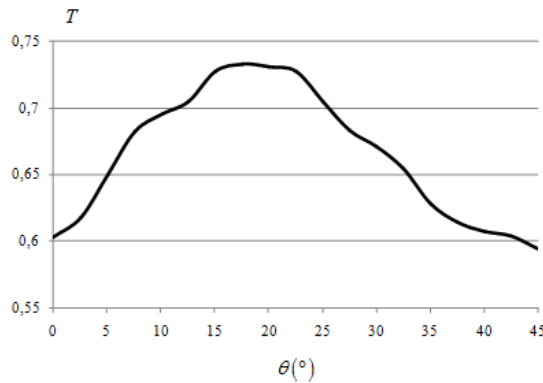**Figure 9.** $b^{s*}_{n(p)}$ for $r^s_t = 0.5$ and $r^r_t = 0.8$ for rectangular slots.

Figure 10. $b^{g*}_{(Q)}$ for $r^s_t = 0.5$ and $r^r_t = 0.8$ for rectangular slots.

slotting resonance harmonics when $r^s_t = 0.5$ and $r^r_t = 0.8$, are thus checked numerically on rectangular shape slots. Considering now the case of the semi-closed slots. Here, the simulation is performed with a non linear material because as previously mentioned, the horn part of the slot is saturated. Fig. 11 and Fig. 12 give $b^{s*}_{n(P)}$ respectively for $r^s_t = r^r_t = 0.8$ and for $r^s_t = 0.5$, $r^r_t = 0.8$. The slotting resonance phenomenon is still visible in Fig. 11, but the theoretical optimal value of r^s_t does not lead to a full cancellation of the harmonics as presented in Fig. 12. A residual value still exists. The numerical analysis shows that a minimization of the dynamic iron losses is still possible in case of real shape slots associated with saturation effect, but a more accurate adjustment of the geometrical parameters is necessary to optimize the cancellation of slotting resonance harmonics.
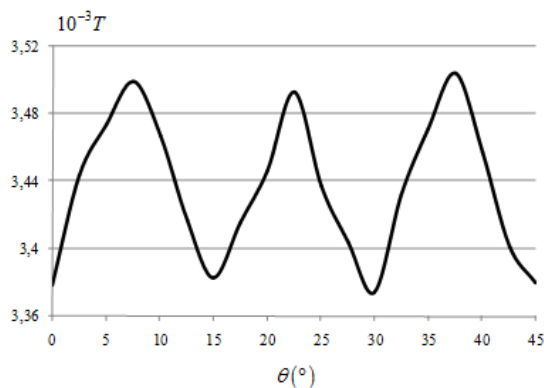
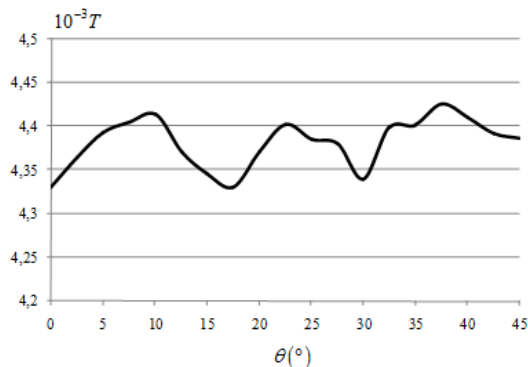**Figure 11.** $b_{n(P)}^{s*}$ for $r_t^s = r_t^r = 0.8$ for semi-closed slots.

Figure 12. $b_{n(P)}^{s*}$ for $r_t^s = 0.5$ and $r_t^r = 0.8$ for semi-closed slots.

6. CONCLUSION

A semi analytical model of the machine that combines an air-gap **FD** model, a core **FD** repartition model and an iron losses model is presented. It has been shown that the stator and rotor slot openings have non negligible effect on the iron losses. These results prove that the judicious choice of these parameters when designing a machine is important to minimize the iron losses due to the **FD** harmonics and thus to minimize the total iron losses. A numerical study using finite element method has been carried out on two slots shapes to validate theoretical results. This numerical analysis confirms the cancellation of slotting resonance harmonic **FD** for some stator and rotor slotting ratio values and hence the minimization of the iron losses due to the slotting harmonics. The use of real shape semi-closed slot influences

the results but the property is still valid. Further works consist in researching an equivalent suitable stator and rotor slotting ratio for this kind of slots geometry.

REFERENCES

1. Ma, L., M. Sanada, S. Moromoto, and Y. Takeda, "Iron loss prediction considering the rotational field and flux density harmonics in IPMSM and SynRM," *IEE Proc. — Electr. Power Appl.*, Vol. 150, No. 6, 747–751, Nov. 2003.

2. Bottruscio, O., M. Chiampi, A. Manzin, and M. Zucca, "Additional losses in induction machines under synchronous no-load conditions," *IEEE Trans. on Magnetics*, Vol. 40, No. 5, 3254–3261, Sep. 2004.

3. Diaz, G., P. Arboleya, C. Gonzalez-Moran, and J. Gomez-Aleixandre, "Revision of the hysteresis and excess loss computation method as a means of improving the rotational loss estimate in induction motors," *IET Elecr. Power Appl.*, Vol. 1. No. 1, 75–81, Jan. 2007.

4. Lee, J. J., Y. K. Kim, H. Nam, K. H. Ha, J. P. Hong, and D. H. Hwang, "Loss distribution of three phase induction motor fed by pulsewidth modulated inverter," *IEEE Trans. on Magnetics*, Vol. 40, No. 2, 762–765, Mar. 2004.

5. Gmyrek, Z., A. Boglietti, and A. Cavagnino, "Estimation of iron losses in induction motors: Calculation, method, results, and analysis," *IEEE Trans. on Industrial Electronics*, Vol. 57, No. 1, 161–171, Jan. 2010.

6. Cassoret, B., R. Corton, D. Roger, and J. F. Brudny, "Magnetic noise reduction of induction machine," *IEEE Trans. on Power Electronics*, Vol. 18, No. 2, 570–579, Mar. 2003.

7. Le Besnerais, J., V. Lanfranchi, M. Hecquet, R. Romary, and P. Brochet, "Optimal slot opening width for magnetic noise reduction in induction motors," *IEEE Trans. on Energy Conversion*, Vol. 24, No. 4, 869–874, Dec. 2009.

8. Yamazaki, K., "Harmonic copper and iron losses calculation of induction motor using nonlinear time-stepping finite element method," *IEEE International Electric Machines and Drives Conference*, 551–553, Cambridge, Massachussetts, USA, Jun. 2001.

9. Brudny, J. F. and R. Romary, "Analysis of the slotting effect on the induction machine dynamic iron losses," *Computer Fields Models of Electromagnetic Devices*, IOS Press, Vol. 34, 27–73, 2010.

10. Lopez, S., B. Cassoret, J. F. Brudny, L. Lefebvre, and J. N. Vincent, "Grain oriented steel assembly characterization for the development of high efficiency AC rotating electrical machines," *IEEE Trans. on Magnetics*, Vol. 45, No. 10, 4161–4164, Oct. 2009.

11. Brudny, J. F., B. Cassoret, R. Lemaitre, and J. N. Vincent, "Magnetic core and use of magnetic core for electrical machines," International Patent PCT/EP2008/061884, Mar. 2009.

12. Carter, F. W., "Air gap induction," *Electrical World*, Vol. 38, 884–892, 1901.

13. Romary, R., D. Roger, and J. F. Brudny, "Analytical computation of an AC machine external magnetic field," *European Physical Journal — Applied Physics EPJ-AP, EDP Sciences*, Vol. 47, No. 3, Paris, Sep. 2009.

14. Thailly, D., R. Romary, D. Roger, and J. F. Brudny, "Attenuation of magnetic field components through an AC machine stator," *ISEF 2007*, No. 38, Prague, CD ROM, 2007.

15. Bertotti, G., "General properties of power losses in soft ferromagnetic materials," *IEEE Trans. on Magnetics*, Vol. 24, No. 1, 621–630, 1988.

16. Boglietti, M. A., A. Cavagnino, M. Lazzari, and M. Pastorelli, "Predicting iron losses in soft magnetic materials with arbitrary voltage supply: An engineering approach," *IEEE Trans. on Magnetics*, Vol. 39, 981–989, Mar. 2003.

17. Ranlof, M., A. Wolfbrandt, J. Lidenholm, and U. Lundin, "Core loss prediction in large hydropower generators: Influence of rotational fields," *IEEE Trans. on Magnetics*, Vol. 45, No. 8, 3200–3206, Aug. 2009.

18. Bottauscio, O., A. Canova, M. Chiampi, and M. Repetto, "Iron losses in electrical machines: Influence of different material model," *IEEE Trans. on Magnetics*, Vol. 38, No. 2, 805–808, Mar. 2002.

19. Deng, F., "An improved iron loss estimation for permanent magnet brushless machines," *IEEE Trans. on Energy Conversion*, Vol. 14, No. 4, 1391–1395, Dec. 1999.

20. Roger, A. N., "Prediction of loss in silicon steel from distorted waveform," *IEEE Trans. on Magnetics*, Vol. 14, No. 4, 263–268, Jul. 1978.

21. Brudny, J. F., "Modelling of induction machine slotting resonance phenomenon," *European Physical Journal Applied Physic*, 1009–1023, JP III, May 1997.